Regulation of Tyrosyl-DNA Phosphodiesterase 2 (TDP2) by Poly-Ubiquitin

Matthew J. Schellenberg, C. Denise Appel, Amanda A. Riccio, Logan R. Butler, Juno M. Krahn, Jenna A. Liebermann, Felipe Cortés-Ledesma, and R. Scott Williams

Supplementary Figures 1–8.
Supplementary Tables 1–3.

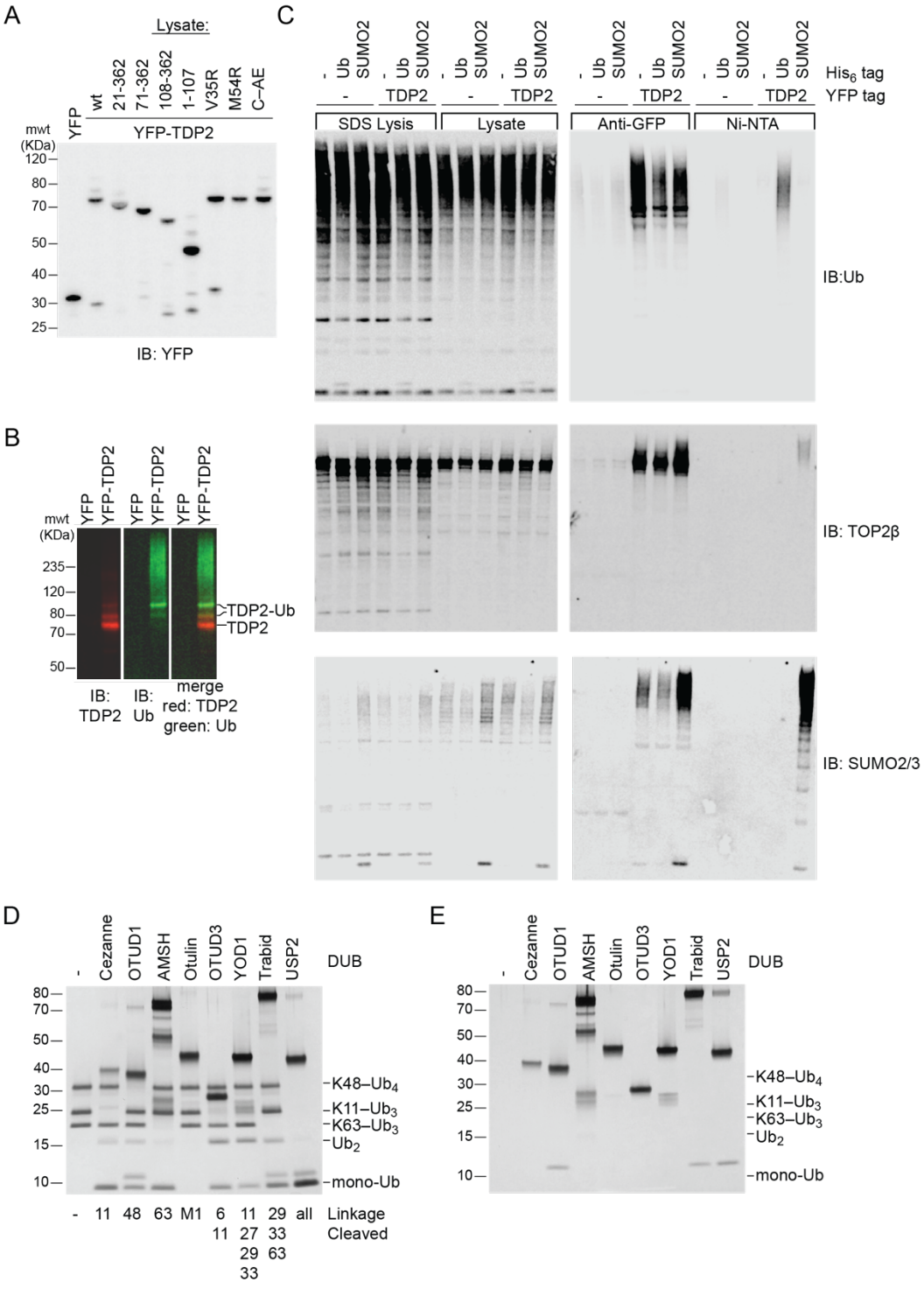

Supplementary Figure 1. Immunoprecipitation of TDP2 mutants. (A) Lysates from cells expressing the indicated YFP-tagged proteins were run on an SDS-PAGE and immunoblotted with anti GFP/YFP. (B) An immunoblot of immunoprecipitated YFP and YFP-TDP2 was probed with rabbit anti-TDP2/anti-rabbit IRDYE680 (red) and mouse anti-Ub/anti-mouse IRDYE800 (green). Two ubiquitinated TDP bands that co-stain with both antibodies are present. (C) Immunoblot of lysates, soluble lysates, anti-GFP eluate, and Ni-NTA purified samples from cells expressing YFP/YFPTDP2 and His_6-SUMO2/His_6-Ub. (D) Silver-stained SDS-PAGE of reactions containing 100 nM of each K48–Ub_4, K11-Ub_3, and K63-Ub_3 after incubation with the indicated DUBs. The linkage type hydrolyzed by each DUB is indicated under the gel. Compare to (E) reactions containing only the DUB to identify non-ubiquitin bands present in the DUB enzymes.

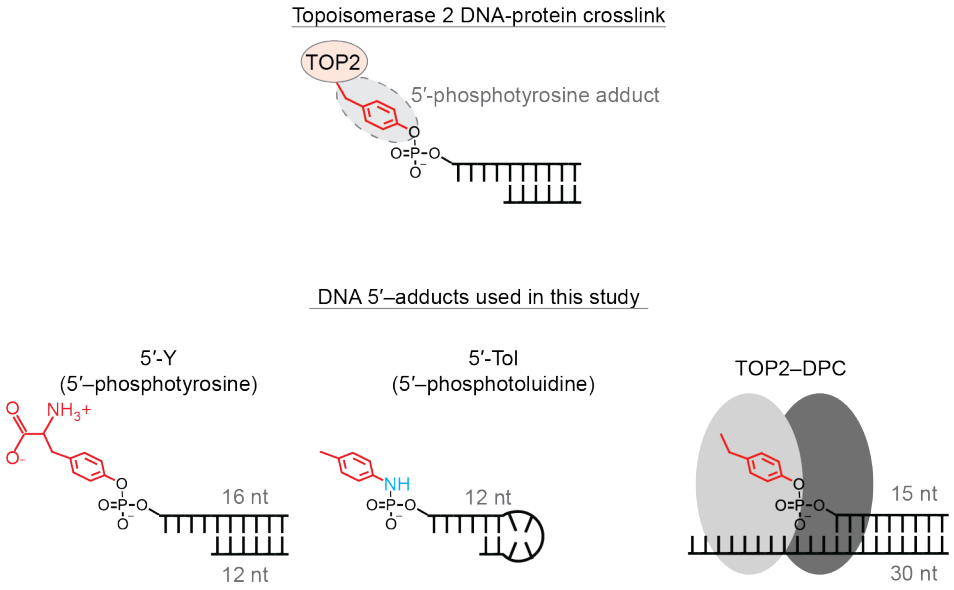

Supplementary Figure 2. TDP2 substrates used in this study.

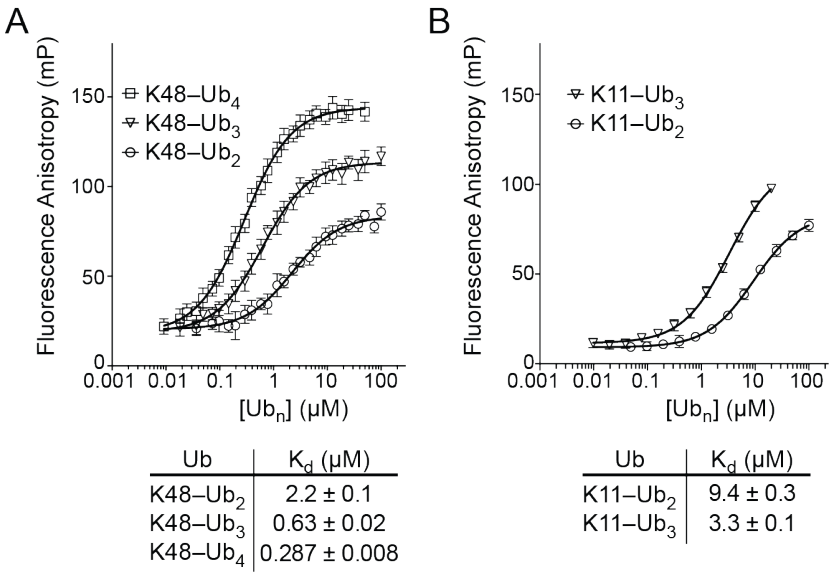

Ub	K_d (μM)
$K48–Ub_2$	2.2 ± 0.1
$K48–Ub_3$	0.63 ± 0.02
$K48–Ub_4$	0.287 ± 0.008

Ub	K_d (μM)
$K11–Ub_2$	9.4 ± 0.3
$K11–Ub_3$	3.3 ± 0.1

Supplementary Figure 3. UBA binding affinities for K48 and K11 Ub chains. Fluorescein-UBA protein was incubated with increasing amounts of the indicated (A) K48–Ub or (B) K11–Ub chains and the FP value was measured at each concentration. Error bars, S.D. N=4 replicates. Data were fit to single binding-site model (solid line) to calculate Kd values ±s.e.m.

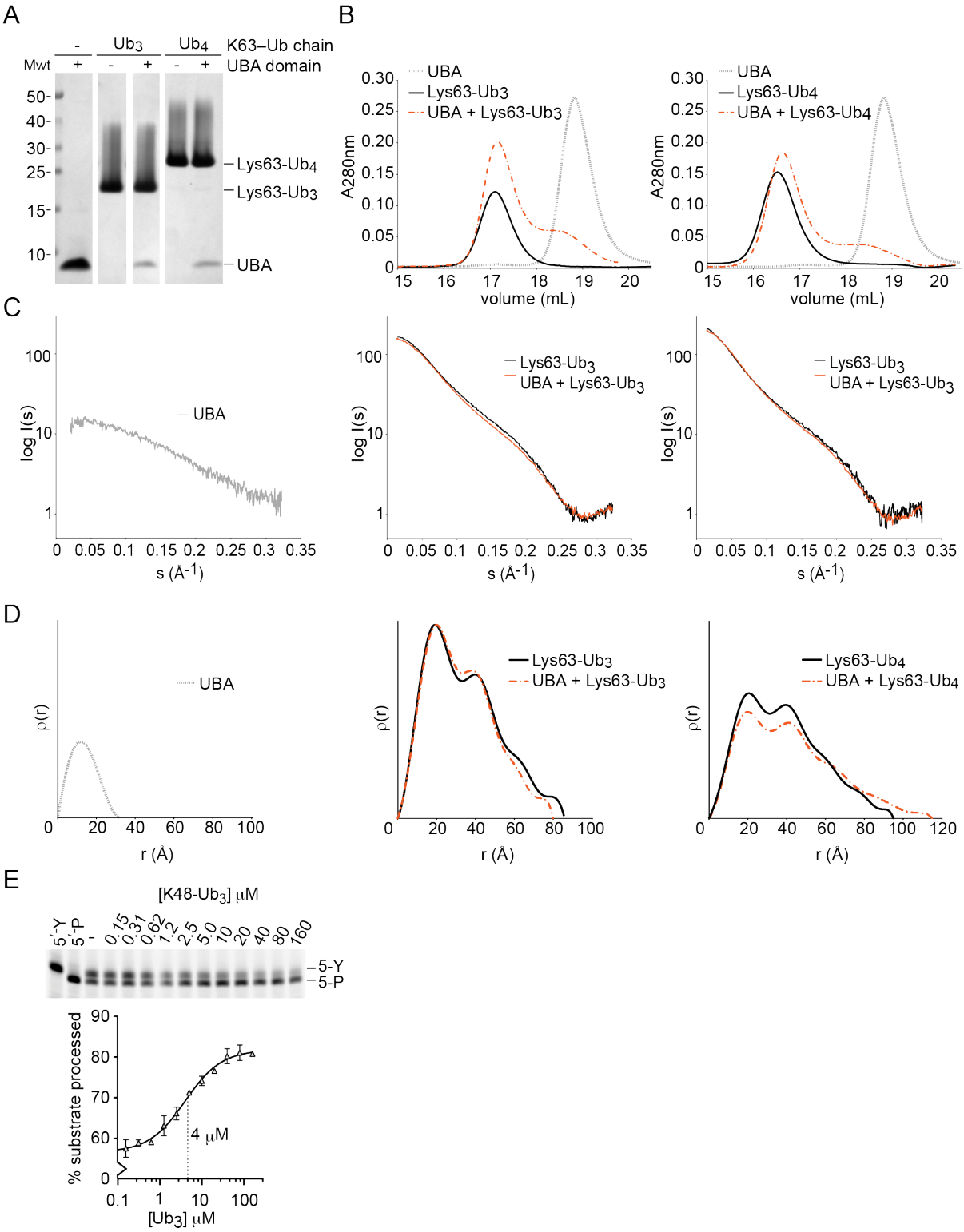

Supplementary Figure 4. SAXS analysis of UBA:poly–Ub complexes. (A) SDS-PAGE of FPLC purified UBA and K63–Ub proteins used for SAXS data collection. (B) UBA, K63–Ub_n, or a mixture of both proteins were run on an S200 10/300 size exclusion column. The complex of UBA: K63–Ub_n elutes later than K63–Ub_n alone, suggesting that the complex is more compact than K63–Ub_n. (C) SAXS plot of scattered intensity for the indicated proteins. (D) $\rho(r)$ plots for the indicated proteins were calculated from the measured scattering intensity, and indicate that the UBA: K63–Ub_n complexes are more compact than the corresponding K63–Ub_n. (E) . (upper) Recombinant TDP2 protein and the indicated [K48–Ub_3] chains were incubated with 5′–phosphotyrosyl DNA substrate. Detyrosylation of the DNA was monitored by denaturing PAGE. (lower) % of product DNA formation on PAGE gels was plotted as a function of

Ubiquitin concentration, and data were fit to a dose-response model (solid line) to determine EC50 values. Error bars, S.D. N=3 replicates.

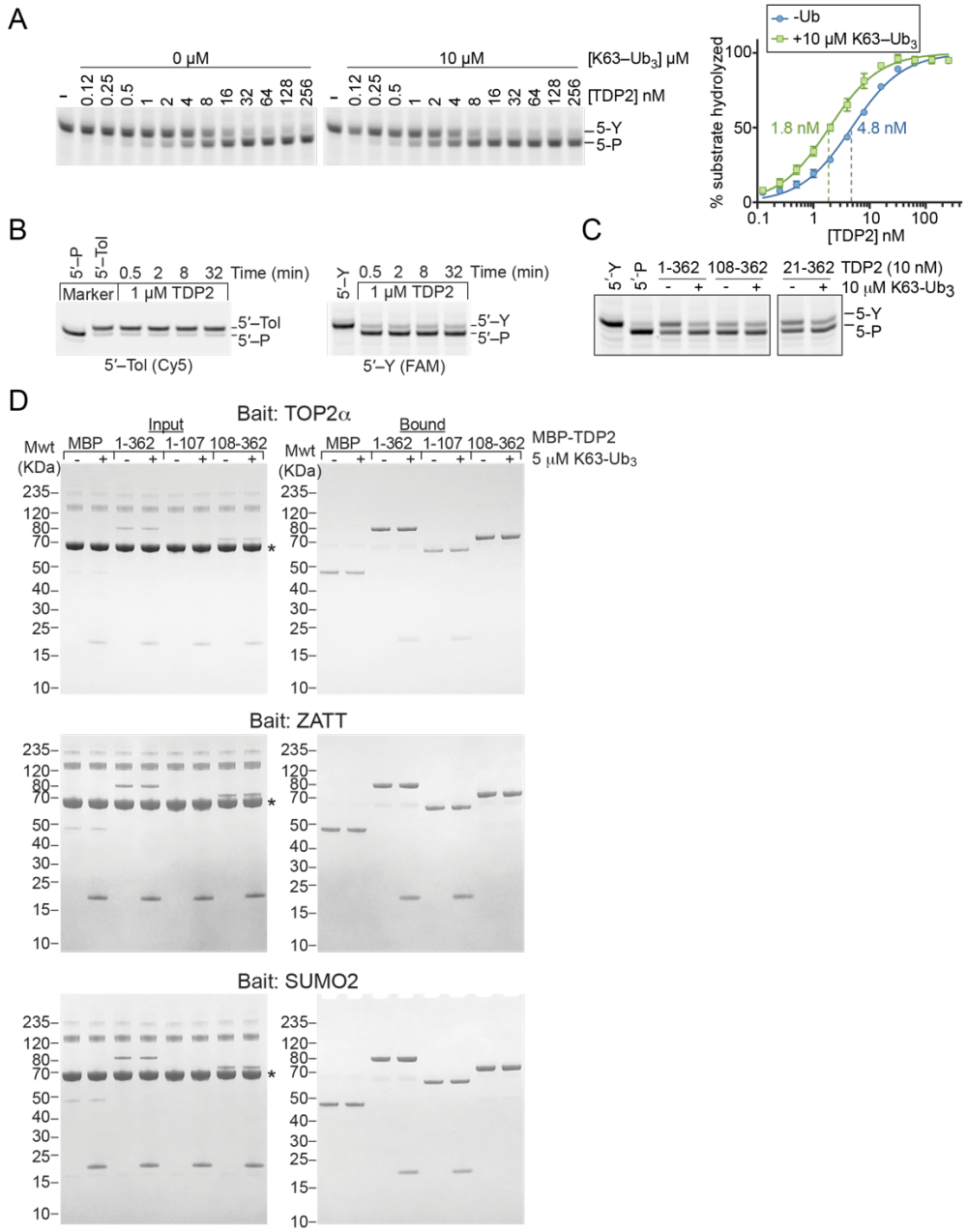

Supplementary Figure 5. K63–Ub$_3$ regulates TDP2. (A) Stimulation of TDP2 catalytic activity by K63–Ub$_3$ chains. (left) Recombinant TDP2 protein with K63–Ub$_3$ where indicated were incubated with 5′–phosphotyrosyl DNA substrate. Detyrosylation of the DNA was monitored by denaturing PAGE. (right) % of product DNA formation on PAGE gels was plotted as a function of TDP2 concentration, and data were fit to a dose-response model (solid line) to determine EC$_{50}$ values. Error bars, S.D. N=3 replicates. (B) TDP2 does not hydrolyze 5′–Tol DNA. 1 μM TDP2 was incubated in reactions that contained 5 nM 5′–Tol (Cy5) and 500 nM 5′–Y (FAM) DNA for the indicated times, and hydrolysis was monitored by denaturing PAGE. 5′–Y DNA is hydrolyzed before the first timepoint, while 5′–Tol DNA is unaffected by TDP2. (C) TDP2 or truncated mutants were incubated with 5′–Y DNA and K63–Ub$_3$ where indicated. Reaction products were analyzed by denaturing PAGE. Representative gel of three replicate experiments is shown. (D) K63–Ub$_3$ regulates the interaction between TDP2 and TOP2α and ZATT. The effect of K63–Ub$_3$ on the interaction between TOP2α, ZATT, or SUMO2 and MBP–TDP2 fusion proteins was assayed using an

in vitro pulldown assay. Coomassie blue stained SDS–PAGE of input and resin–bound fractions shows equal loading and recovery of MBP proteins. *= BSA (Bovine Serum Albumin) included in the assay to protect against non-specific interactions.

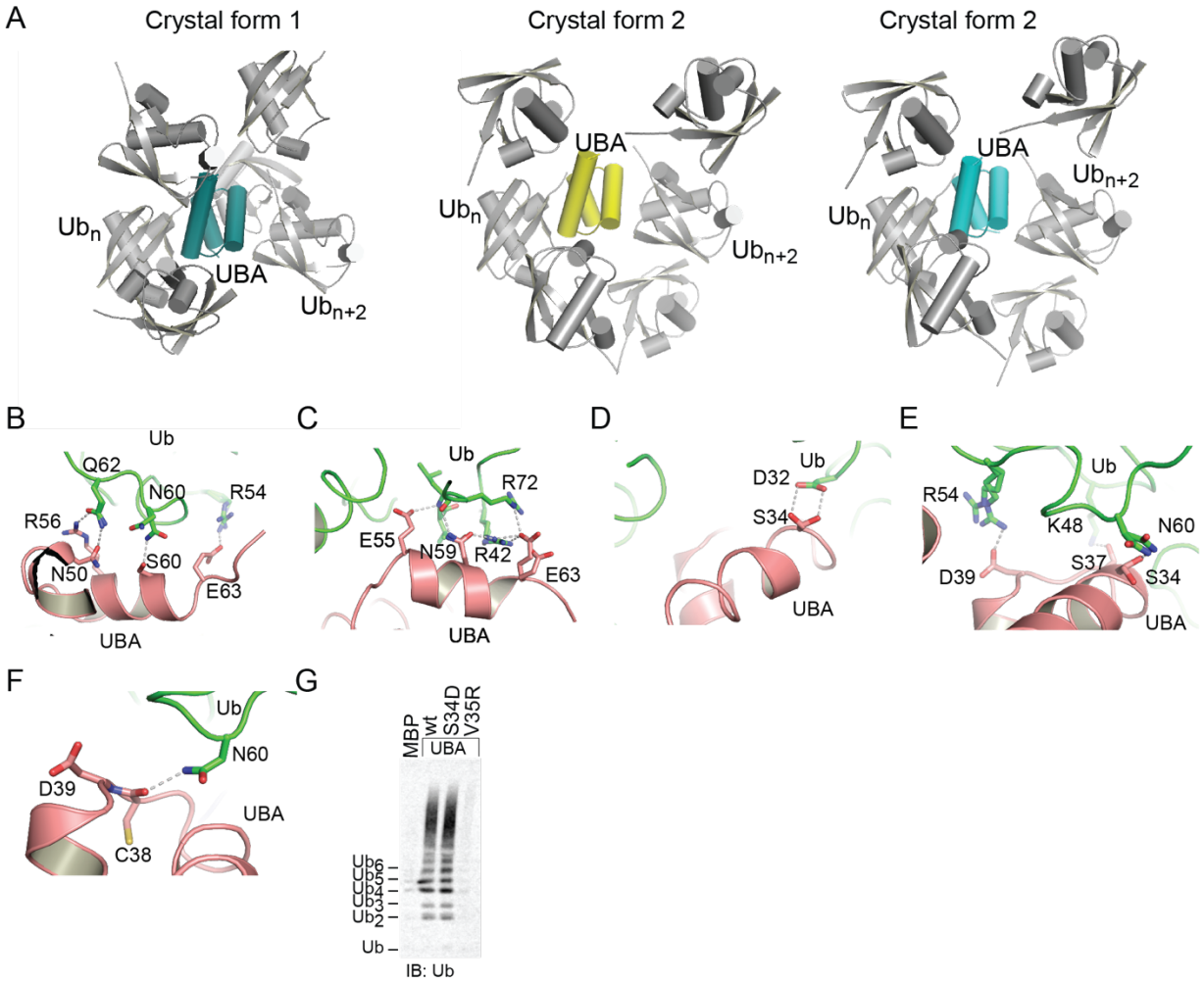

Supplementary Figure 6. Analysis of crystal lattice and conserved sequences of the UBA domain. (A) Location of Ub monomers within 4Å of the UBA domain in the indicated crystal forms. (B) Crystal form 1 has a crystal pack consisting of the indicated hydrogen bonds, but is unlikely to contribute to poly–Ub since S60R does not alter poly–Ub binding (Fig. 6C), and this interface is not found in Crystal form 2. (C) In crystal form 2, E63 forms a different set of hydrogen bonds to R42 and R72 of Ub. N59 makes a backbone hydrogen bond to Ub, but is unlikely to contribute to poly–Ub since N59D does not alter poly–Ub binding (Fig. 6C). (D) Crystal form contains a hydrogen bond between two alternate conformations of S34 and D32, but is unlikely to contribute to poly–Ub binding since S34D does not impact poly–Ub binding (panel G), and crystal form 2 does not contain the same interface. (E) In crystal form 2, S34 hydrogen bonds to Ub N60, with additional hydrogen bonding from UBA D39 to Ub R54. This interface is unlikely to contribute to poly–Ub since D39G and S34D do not alter poly–Ub binding (Fig. 6C). (F) A small interface consisting of a single hydrogen bond between Ub N60 and the backbone carbonyl of UBA C38 is found in one monomer of crystal form 2, but not the other or crystal form 1. (G) Western blot analysis of K63 poly–Ub chains bound to mutant MBP-UBA proteins in an in vitro pull down assay.

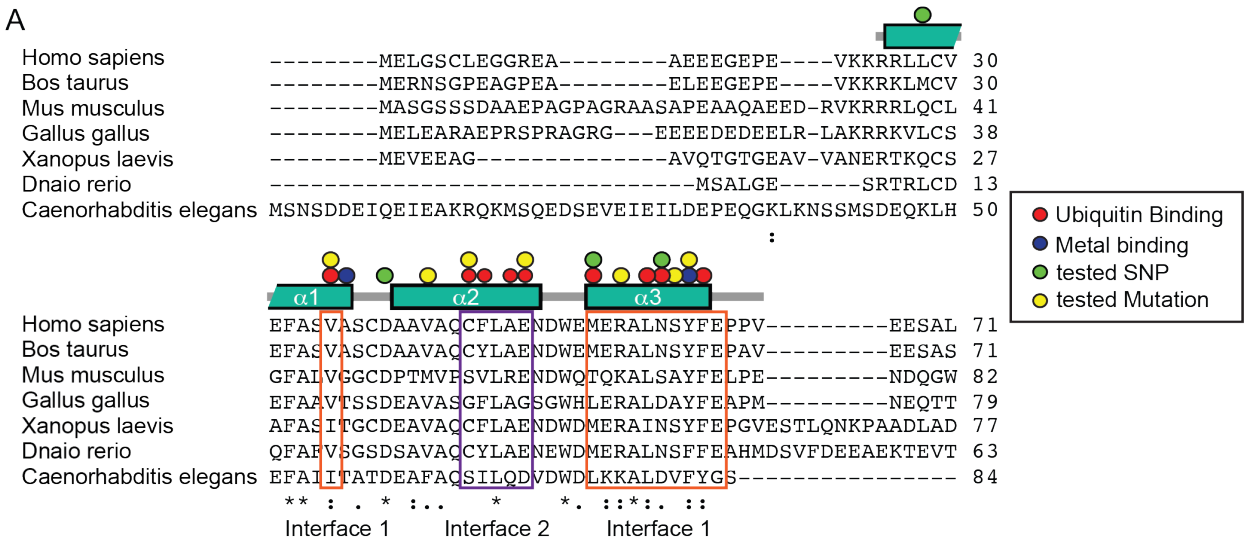

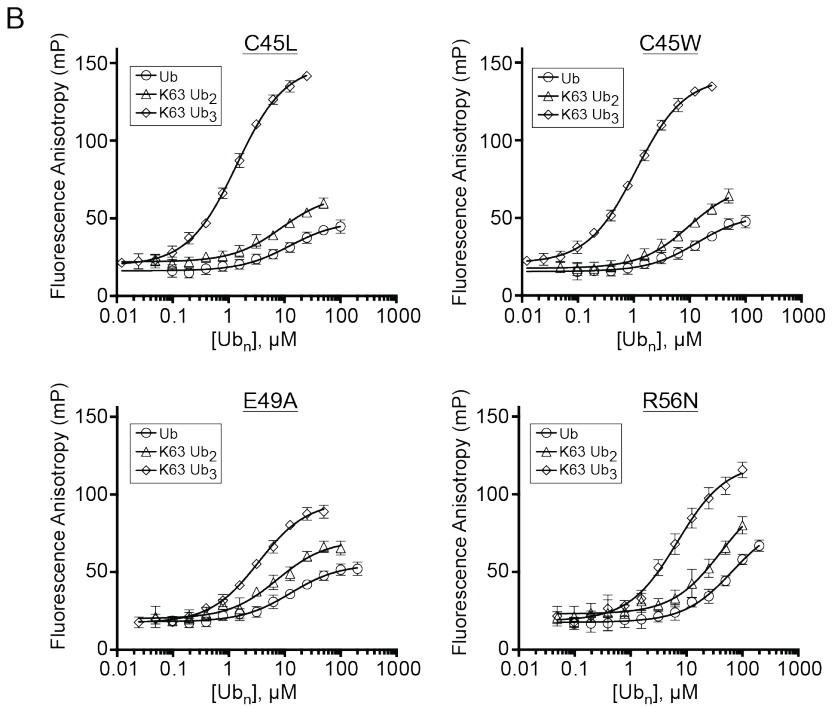

	K_d ± s.e.m. (μM)		
UBA protein	Mono-Ub	K63–Ub_2	K63–Ub_3
WT (Fig. 2C)	11 ± 1	8.3 ± 0.5	0.77 ± 0.03
C45L	12 ± 2	8.7 ± 0.9	1.39 ± 0.04 **
C45W	13 ± 2	9.7 ± 0.9	1.10 ± 0.03**
E49A	13 ± 1	7.3 ± 0.7	3.4 ± 0.2**
R56N	~66	~41	6.9 ± 0.4**

Supplementary Figure 7. Effect of UBA mutations on affinity for Ubiquitin. (A) Sequence alignment of TDP2 homologs. (B) N-terminally fluorescein-labeled TDP2-UBA (aa 25-66) protein containing the indicated mutations was incubated with increasing amounts of the indicated Ub or Ub chain in quadruplicate, and the Fp value at each concentration was measured four times. error bars s.d. Data were fit to a single-site binding model to calculate K_d values. ** $p<0.001$, Extra sum-of-squares F-test compared to WT UBA K_d.

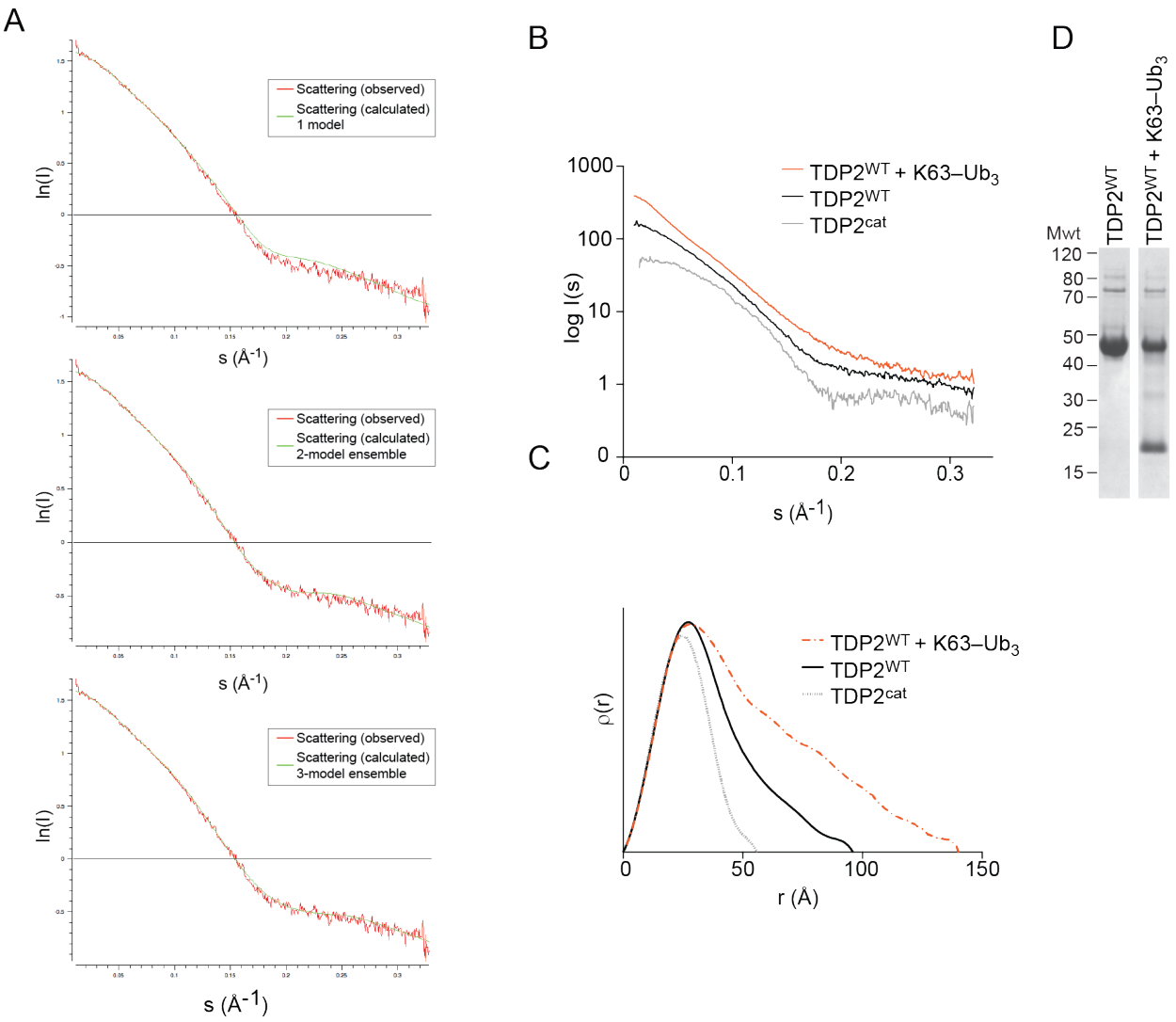

Supplementary Figure 8. SAXS analysis of TDP2:K63–Ub$_3$ complexes. (A) Comparison of observed scattering and calculated scattering of EOM models (B) SAXS plot of scattered intensity for the indicated proteins. (C) ρ(r) plots for the indicated proteins were calculated from the measured scattering intensity, and indicate that the TDP2:K63–Ub$_3$ complex forms an extended conformation that is greater than the length of TDP2 alone. (D) SDS-PAGE of purified TDP2 and TDP2:K63–Ub$_3$ samples used for SAXS data collection.

proteins	Mass (KDa)	R_g (Guinier)	D_{max}	R_g (real space)
UBA	5	10.4	32	10.4
K63–Ub_3	26	26.7	85	27.3
UBA + K63–Ub_3	31	25.0	80	25.7
K63–Ub_4	34	32.4	115	33.6
UBA + K63–Ub_4	39	29.7	95	30.1
TDP2 100 mM NaCl	41	25.6	84	25.6
TDP2 200 mM NaCl	41	27	94	16.7
TDP2 300 mM NaCl	41	29	102	29.3
TDP2 500 mM NaCl	41	30	110	31.3
TDP2 750 mM NaCl	41	34	125	35.4
TDP2 108-362	29	19.9	56	20.3
TDP2:K63–Ub_3	67	42.5	140	42.6

Supplementary Table 1. Molecular parameters derived from SAXS data for the indicated protein or co-purified protein complexes. Data were collected in buffer containing 300 mM NaCl unless otherwise indicated.

	UBA–Ub Form 1	UBA–Ub Form 1 anomalous	UBA–Ub Form 2	UBA–Ub Form 2 anomalous
Data collection				
Space group	$P4_1$	$P4_1$	$p2_12_12_1$	$p2_12_12_1$
Cell dimensions				
a, *b*, *c* (Å)	48.74, 48.74, 50.42	48.65, 48.65, 50.77	53.79, 65.46, 67.68	54.00, 65.52, 67.49
α, β, γ (°)	90, 90, 90	90, 90, 90	90, 90, 90	90, 90, 90
Wavelength (Å)	0.8266	1.541	0.8211	1.541
Resolution (Å)	50-0.85 (0.86-0.85)	50-1.71 (1.74-1.71)	50-0.85 (0.86-0.85)	50-1.60 (1.63-1.60)
R_{merge}	0.049 (1.242)	0.029 (0.068)	0.081 (0.852)	0.027 (0.080)
$I / \sigma I$	59.3 (1.6)	131.3 (23.1)	20.7 (1.3)	153.7 (25.8)
$CC_{1/2}$	1.000 (0.571)	1.000(0.996)	0.987 (0.501)	0.999 (0.997)
Completeness (%)	99.6 (97.8)	99.2 (86.1)	98.5 (84.5)	93.1 (59.6)
Redundancy	16.1 (8.6)	24.5 (6.8)	5.3 (3.0)	31.8 (23.7)
Wilson B–factor	10.6	12.3	10.0	16.6
Refinement				
Resolution (Å)	28.4-0.85		28.0-0.85	
No. reflections	102957		205423	
Min. F/σF	1.34		1.34	
R_{work} / R_{free}	0.095/0.112		0.101/0.114	
No. atoms (non-H)				
Protein	1245		2400	
Ligand/ion	2		18	
Water	233		570	
B factors (Å^2)				
Protein	12.8		12.8	
Ligand/ion	15.2		14.0	
Water	21.8		22.4	
Ramachandran plot:				
Favored (%)	100		100	
Allowed (%)	0		0	
Outliers (%)	0		0	
r.m.s. deviations				
Bond lengths (Å)	0.013		0.010	
Bond angles (°)	1.47		1.39	

All data was collected from a single crystal.
*Values in parentheses are for highest-resolution shell (5% of reflections).

Supplementary Table 2. X-ray crystallography data collection and refinement statistics.

Number of models	Chi-value
1	0.477
2	0.454
3	0.447
4	0.448
5	0.448
10	0.448
20	0.449
unrestrained	0.448

Supplementary Table 3. **Comparison of TDP2 model pools generated by EOM to measures solution X-ray scattering.** EOM compares ensembles with the indicated pool size selected by the genetic algorithm to the experimentally measured SAXS data.